Broadband Sound Radiated from Subsonic Rotors[1]

C. L. MORFEY

Institute of Sound & Vibration Research
University of Southampton, England

Recent theoretical work on sound sources in subsonic turbomachinery is applied to the correlation of axial-flow fan and compressor noise measurements. Correlations are presented for directivity and sound-power spectra associated with broadband noise. A simple explanation is given to account for the relative amounts of sound power transmitted upstream and downstream from a single-stage fan.

The mechanisms of sound generation in subsonic turbomachinery are understood in principle and have been documented in a recent paper by the author (ref. 1). Current fundamental research is now aimed at describing the unsteady flow within the machine with sufficient accuracy that the relative importance of the various mechanisms can be assessed.

Existing noise measurements are unfortunately not matched by the necessary unsteady aerodynamic measurements; in this situation, positive identification of mechanisms is clearly not possible. Any correlation of data with mean-flow measurements will remain of doubtful generality until the gap is closed.

If a particular noise-generation mechanism is put forward as a hypothesis, however, theory can provide considerable guidance in the correlation of measurements. Even though only mean-flow aerodynamic measurements are available, the relevant unsteady-flow components can be related to the steady flow by similarity arguments. Considerable success has been achieved in this way in jet noise correlation, following the initial work of Lighthill (ref. 2); the same approach is adopted in this paper for broadband fan noise.

---

[1] The cooperation of Rolls-Royce Limited in supplying data is gratefully acknowledged. The initial calculations were carried out by R. Snow, B.A.C. Acoustics Laboratory, Weybridge, while at I.S.V.R., Southampton University.

Following the studies by Smith and House (ref. 3) and Morfey and Dawson (ref. 4) on aircraft-engine fan and compressor noise, further data on broadband noise have become available covering a range of axial-flow machines (table I). These are reported by Snow in reference 5, which gives details of measurement and analysis techniques and forms the basis of the present study.

In the sections that follow, various aspects of the noise measurements—sound-power spectrum shapes and levels, directivity patterns and the ratio of downstream to upstream radiated power—are discussed and correlated with mean-flow data. The theory on which the correlations are based has been developed where necessary in the appendixes.

CORRELATION OF BROADBAND POWER SPECTRUM SHAPES

The correlation of broadband sound-power spectra is approached in two stages. First, a frequency parameter is sought that brings the different spectra into line horizontally; then, for a fixed value of the frequency parameter, normalized values of sound-power spectral density are plotted versus Mach number. This is the same general procedure as was followed by Smith and House (ref. 3), although the details differ.

Nondimensional Frequency Parameter

Given a characteristic length scale L, a nondimensional frequency parameter can be formed either as a Strouhal number fL/U, where U is a characteristic velocity, or as the ratio fL/c $(=L/\lambda)$. These are related by the Mach number U/c.

We start by choosing a length scale, leaving till later the choice between U and c as velocity scales. It is expected that the spectrum of broadband sound radiated from a rotor-stator stage will depend on the scale of turbulence in the rotor wake. This in turn is related to the rotor wake-momentum thickness, as Mugridge has shown (ref. 6).

A possible length scale is therefore $b_R C_D$ (equal to twice the momentum thickness), where b_R is the first-rotor chord and C_D is the profile drag coefficient. This may conveniently be estimated in terms of the irreversible temperature rise ΔT_{irr} through the first rotor (ref. 7):

$$b_R C_D \doteq \frac{(\Delta T)_{\text{irr}}}{T_{01}} \cdot \frac{2\, d_R \cos \beta_2}{(\gamma - 1) M_R^2} \qquad (1)^2$$

In equation (1), $d_R \cos \beta_2$ represents the rotor wake spacing and M_R is the relative Mach number at the rotor exit.

---

[2] $(\Delta T)_{\text{irr}}$ is assumed small compared with the stagnation temperature T_{01} at exit from the first rotor.

TABLE I.—*Summarized Compressor Information*

	Type of machine	First rotor			Design point		Blade numbers		
		Hub-tip ratio (entry)	Diameter (in.) (entry)	Mid-Rad. chord, (in.)	Mass flow (lb/s)	Speed (rev/min)	IGV	R1	S1
A	2-stage fan	0.36	45	5.145	370	6 500	24	23	50
B	4-stage fan	0.36	52	4.041	475	5 450		35	52
C_1	7-stage	0.56	25	1.553	84	10 120	37	31	38
C_2	7-stage	0.56	25	1.553	84	10 020	85	31	38
D	8-stage	0.50	17.4	1.680	52	13 760	28	29	28
E	1-stage fan	0.55	24.5	1.815	79	8 550	43	31	50

For the engines tested, information was available on the overall isentropic efficiency η_n and hence on the irreversible temperature rise $(1-\eta_n)(\Delta T_0)_n$ over all n stages. Neglecting stator losses and apportioning the irreversible temperature rise equally between the n rotors gives as a rough estimate

$$(\Delta T)_{\text{irr}} \doteq \frac{1}{n}(1-\eta_n)(\Delta T_0)_n \tag{2}$$

Combining equations (1) and (2) gives a length scale L, defined as

$$L = \frac{2(1-\eta_n)(\Delta T_0)_n}{n(\gamma-1)T_{01}M_R^2} \cdot d_R \cos\beta_2 \tag{3}$$

which because of its link with the wake-momentum thickness should reveal any variations in the eddy scale leaving the first rotor.

This length scale is used below to obtain an empirical collapse of broadband spectrum shapes, with one modification: The rotor relative Mach number is taken for convenience as the inlet (rather than the exit) value. Midradius values are used throughout.

Collapse of Spectrum Shapes

Figure 1 shows, for each engine separately, the collapse of inlet sound-power spectra obtained with $L/\lambda = F$ as frequency parameter. Somewhat surprisingly, this is a good deal better than the collapse obtained with the Strouhal-type parameter F/M_R. Note that the spectra are plotted in constant-percentage-bandwidth form (i.e., the vertical scale is proportional to $f(dW/df)$); the peak occurs around $F=0.1$ to 0.2 in each case. No correction has been made for atmospheric attenuation; the greatest measuring distance was 32 feet.

In figure 2 the mean spectrum shapes from the different engines are superimposed; the broken line for engine B indicates that the horizontal positioning of the spectrum is uncertain since the efficiency had to be estimated from other data. For comparison, figure 2 also shows the mean spectrum shape obtained by Smith and House (ref. 3) for broadband compressor noise at the position of maximum sideline OASPL; the peak has been placed at $F=0.16$ to line up with the present data.[3]

A mean line based on figure 2 lies within 5 dB of most of the data points. Some of the scatter is doubtless due to errors both in sound-power measurement and in the aerodynamic data used for forming the frequency parameter; but the present scheme cannot account for genuine variations in spectrum shape.

---

[3] This implies a value of C_D between 0.1 and 0.2 for the compressors plotted in figure 12 of reference 3.

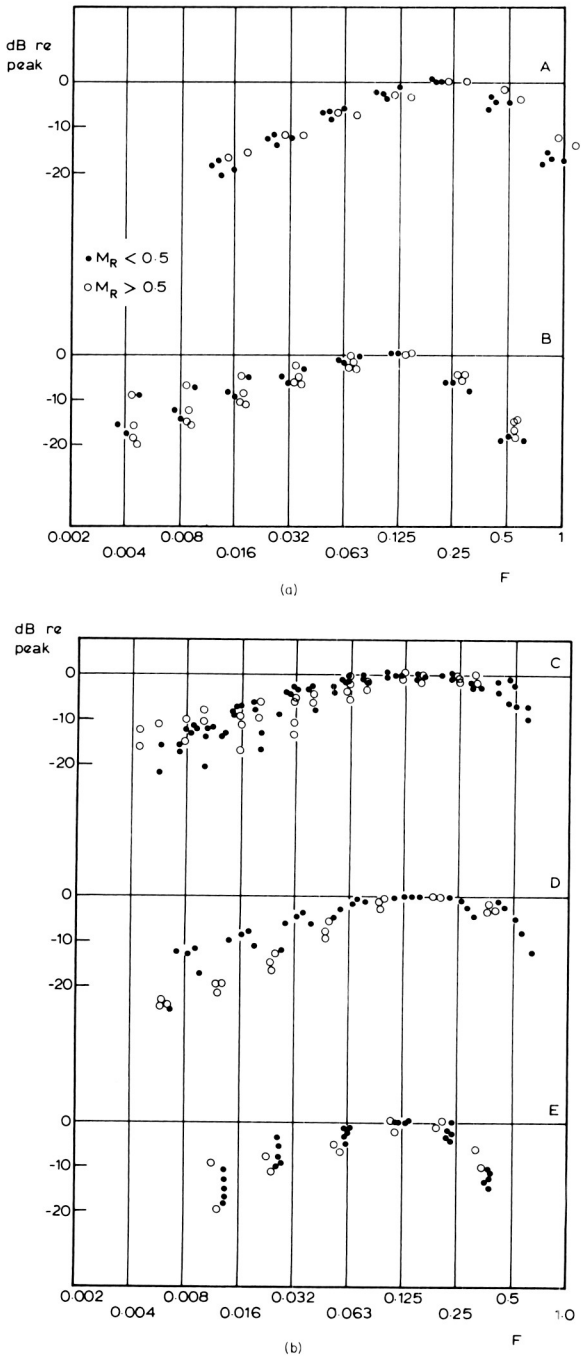

FIGURE 1.—*Spectrum shape correlation—broadband sound power radiated from inlet.*

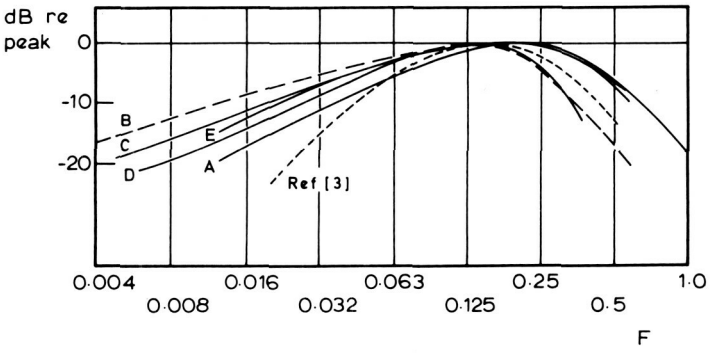

FIGURE 2.—*Mean spectrum shapes for all engines (constant-percentage bandwidth).*

CORRELATION OF ABSOLUTE LEVELS

The next stage in the data correlation process is to collapse the sound-power spectrum levels for a given value of the frequency parameter. This will be done with the aid of a simplified analytical model that predicts the sound-power variation with Mach number, blade area, and other principal factors. A nondimensional sound-power parameter is obtained in which these factors are normalized out; it is found to be constant within ± 5 dB for all the engines measured, up to a rotor inlet Mach number of 0.6.

Nondimensional Sound-Power Parameter

The broadband sound-power spectrum generated by a single rotor-stator stage is related in Appendix I to the characteristics of the rotor wake turbulence. The analysis is highly simplified, its purpose being to predict the main trends so that these can be normalized out from the data. The analysis is based on the following assumptions:

(1) Broadband noise is generated by turbulence from one blade row, entering the row immediately downstream and setting up lift fluctuations on the downstream blades. Only the axial component of the lift fluctuations is taken into account in calculating the sound output (this point will be mentioned again below).

(2) Blade profiles are assumed acoustically compact. (This is a rather crude assumption since the ratio of axial chord to wavelength is of order 1 at the peak of the spectra in figure 1. The effect of noncompact blade profiles on sound radiation requires investigation.)

(3) The axisymmetric rotor-stator geometry is replaced by a two-dimensional model based on mean-radius conditions, and the spanwise

extent of the model is taken as being large compared with the sound wavelength.

(4) The flow is subsonic with $M^2 \ll 1$.

The results of the analysis are summarized in equations (15) and (16) of Appendix I. These involve the unknown quantities l_c (spanwise integral length scale of turbulence) and C_D (rotor-blade drag coefficient), besides the turbulence intensity parameter α. However, if we assume $l_c \propto b_R C_D$, as Mugridge's experiments (ref. 6) indicate, and replace $b_R C_D$ by L as in the previous section, we get the following relationship between the sound-power spectrum and aerodynamic parameters:

$$\frac{f}{\rho c^3 S_R}\frac{dW}{df} \propto M_R{}^5 \left(\frac{f d_R}{c}\right)^{-2} \sigma_S f(\beta_2,\alpha_1) \cdot \alpha \binom{F^3}{F^2} \tag{4}$$

The left-hand side of equation (4) is itself a nondimensional form of the sound-power spectrum; it will be divided by the first four factors on the right-hand side to produce a normalized power parameter.

For this preliminary study, it was considered an advantage to base the normalization solely on rotor parameters; σ_S is therefore replaced by the rotor solidity σ_R, and α_1 is replaced by β_2. Furthermore the C_L term in $f(\beta_2,\alpha_1)$ is neglected. The resulting nondimensional sound-power parameter is

$$G = \frac{dW}{df} \cdot \frac{f^3 d_R{}^2 \csc^4 \beta_2}{\rho c^5 S_R' M_R{}^5} \tag{5}$$

Here $S_R' = \sigma_R S_R$ denotes the rotor blade area (span $\times$ chord $\times$ number of blades). All the quantities that make up G, apart from the sound-power spectrum itself, are generally known at the design stage of a fan or compressor.

As in the previous section, the correlation that follows is based on the relative Mach number at the rotor inlet.[4]

Sound Power Data Correlation

Values of G for $F = 0.16$—corresponding approximately to the peak of the constant-percentage-bandwidth spectra in figure 1—are plotted versus the rotor inlet relative Mach number in figure 3. The data points represent inlet-radiated broadband sound from the six different engines in table I, each run over a range of speeds.

---

[4] Note that for a given F value, $G \propto M_R{}^{-1}$; so the value of G is not very sensitive to the exact definition of M_R, provided the same definition is used in both F and G.

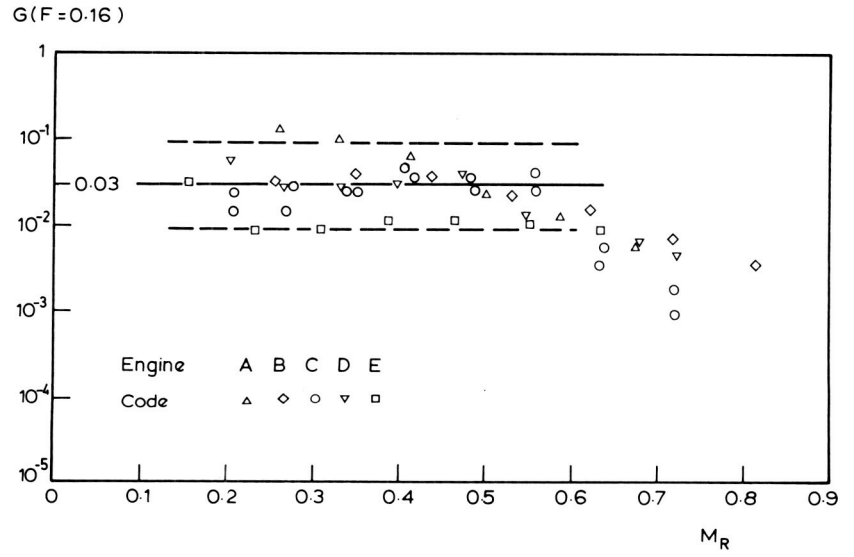

FIGURE 3.—*Sound-power parameter based on peak of spectrum, versus first-rotor inlet relative Mach number.*

Ideally the sound power from each stage would be correlated separately when dealing with a multistage machine. However, there is no way in which the broadband sound output from separate stages can be distinguished when only the total sound output has been measured, as has been done here. The inlet sound-power measurements from the multistage machines (A, B, C, D) have therefore been combined with first-stage rotor parameters to give a value of G. Such a normalization procedure leaves the number of stages unaccounted for, so it is interesting that the single-stage fan tends to fall at the bottom of the scatter band in figure 3 (i.e., about 5 dB below most of the multistage points).

Below $M_R = 0.6$, almost all the points lie within ± 5 dB of the constant value $G = 0.03$; this collapse is encouraging in view of the small number of variables included in the definition of G. Furthermore, the tendency to remain constant over this range of Mach number supports the theoretically predicted M_R^5 variation (see equation (4)).[5]

[5] Note that if the frequency spectrum scaled on relative velocity, rather than the sound speed as indicated in figure 1, the right-hand side of equation (4) for $l_c \ll \lambda$ would be proportional to M_R^6 rather than M_R^5. Although Strouhal number scaling—and hence an M_R^6 dependence for compact sources—is commonly assumed for sound radiation from fluctuating forces of aerodynamic origin, we have shown ("Correlation of Broadband Power Spectrum Shapes") that it does not fit the present data.

Above $M_R = 0.6$, figure 3 shows a falloff in G with increasing M_R; this amounts to roughly 10 dB at $M_R = 0.7$ and is similar to the flow effect found by Smith and House (ref. 3).

DIRECTIVITY OF INLET-RADIATED SOUND

The directivity of broadband inlet-radiated sound is discussed in reference 8; the opportunity is taken here to present an updated correlation due to Snow (ref. 5). In the light of these results, a hypothesis is put forward to account for the directional radiation of broadband sound at high frequencies.

Multistage Data Correlation

Figures 4a and 4b show the directivity index,[6] plotted versus angle from the inlet axis, for five different multistage fans and compressors ($n = 2$ to 8). The parameter is ka, where a is the rms first-rotor radius; each ka curve is based on a number of engine speeds.

At a nondimensional frequency of $ka = 4$, the curves for the various engines collapse within $1\frac{1}{2}$ dB. They also agree fairly closely (up to 60°) with the theoretical curve in figure 5. The latter is taken from reference 8 and represents a spatially random source distribution; the departure from a uniform field shape is due to duct cutoff effects.

At $ka = 16$, the same theoretical model predicts a fairly flat directivity curve, with a slight dip at 90° (fig. 5); but the measured curves fall off a good deal more sharply away from the axis. The departure from the random-source model is still more pronounced at $ka = 63$. In fact, the model predicts hemispherically uniform radiation in the high-frequency limit ($ka = \infty$), while the measured radiation patterns become progressively more directional with increasing frequency above $ka = 4$ and apparently tend toward a $\cos^2 \psi$ directional distribution.[7]

Optical Model for High-Frequency Directivity

A clue to the observed directivity along the axis at high frequencies ($ka = 16$ and above) is provided by closer examination of figure 4. There is a significant trend at 90° for the directivity index to vary according to the number of stages: The higher the number, the larger the dip at 90°. An optical model, outlined below, suggests that reflection of sound by upstream blade rows could account for the observed directivity patterns.

---

[6] Based on the upstream hemisphere ($\psi = 0°$ to 90°); thus omnidirectional radiation has a directivity index of 3 dB.

[7] It is interesting that this is the distribution which corresponds to fluctuating forces oriented in the axial direction.

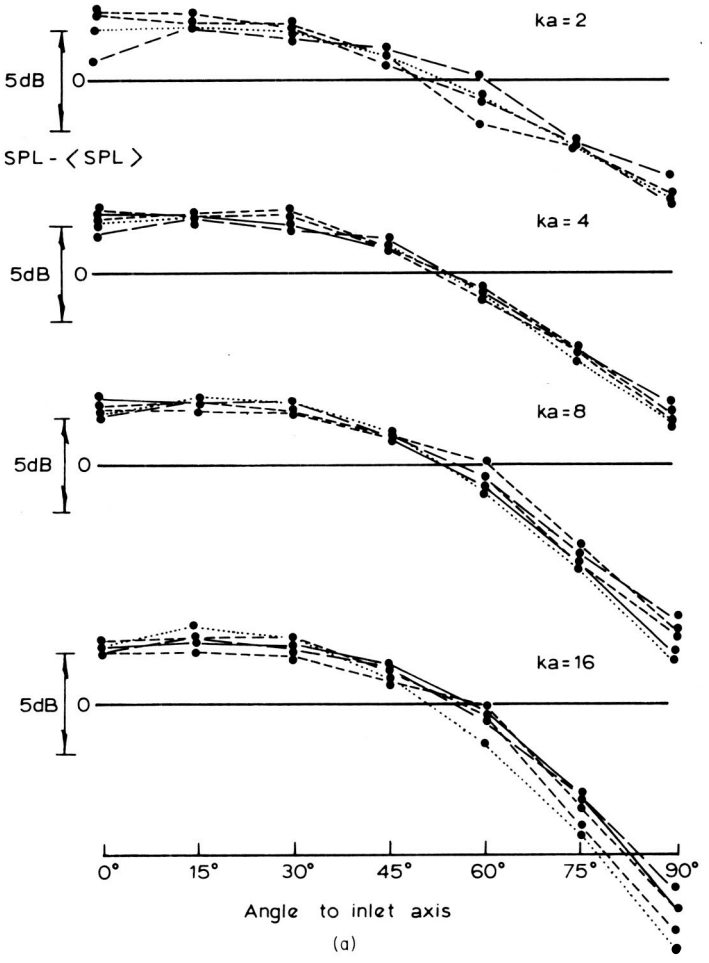

FIGURE 4a.—*Narrowband directivity index measurements for inlet radiation from multistage fans and compressors (frequency band width: 5 percent).*

In a multistage machine, sound generated by the second and subsequent stages must travel through the first stage before it can escape from the inlet. The transmission process is represented in figure 6 by rays that are reflected from the blade surfaces in the same way as light from a mirror; this optical model becomes valid at high frequencies, where the sound wavelength is short compared with the blade chord and spacing.

Referring to figure 6, rays incident on the stator within the shaded band will be reflected back in the downstream direction. The same applies to the rotor, so in this two-dimensional picture the radiation transmitted

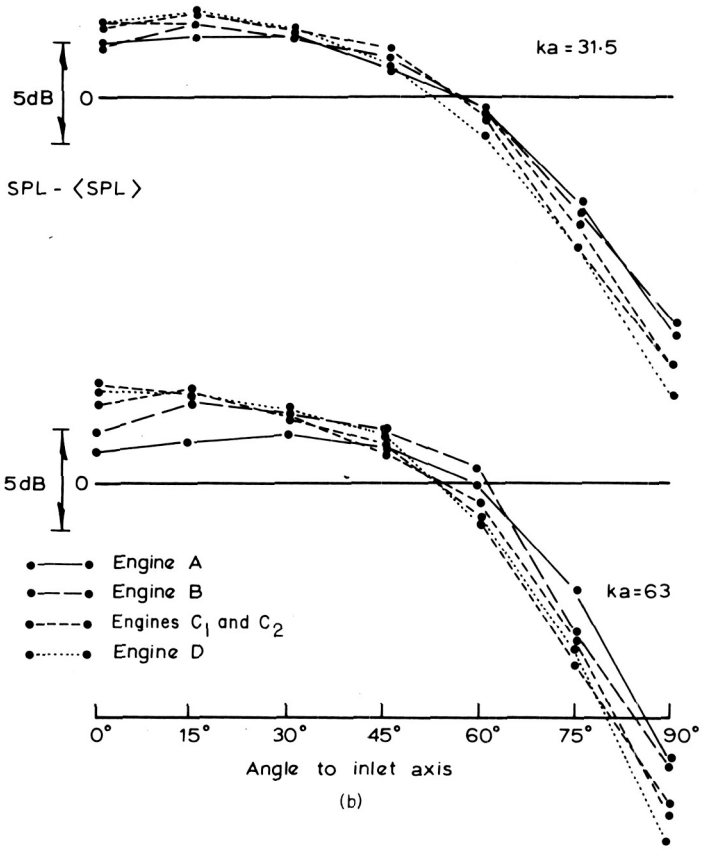

FIGURE 4b.—*Narrowband directivity index measurements for inlet radiation from multistage fans and compressors (frequency bandwidth: 5 percent).*

upstream is confined to a wedge of included angle $\pi-2(\alpha_2'+\beta_2')$.[8] Returning to the three-dimensional geometry of the actual rotor-stator stage, the optical model clearly predicts a reduction of transmitted intensity at 90° (compared with the axial direction) due to upstream blade rows.

This effect probably accounts for at least part of the observed directivity of inlet-radiated noise at $ka=16$ and above. The similarity in figure 4 between the fans A (two-stage) and B (four-stage) may be connected with the absence of IGV's in the latter.

[8] An interesting point is that, if the rotor and stator blade angles add up to more than 90° (which is unusual in aircraft-engine fans and compressors), the model predicts zero sound transmission through this stage.

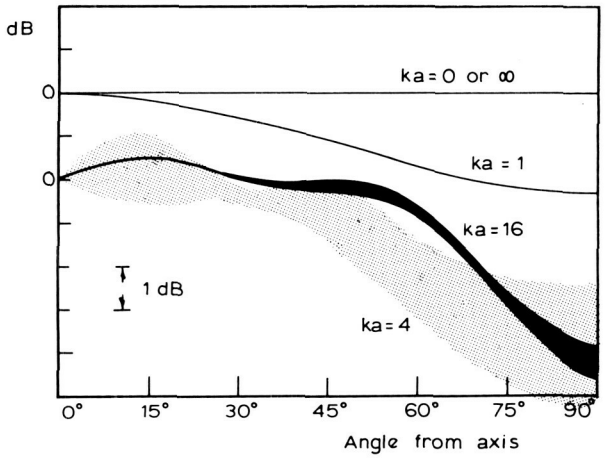

FIGURE 5.—*Theoretical directivity index based on random source model, for* ka = *0 to* ∞. *Bands indicate hub-tip ratio range 0.3–0.5.*

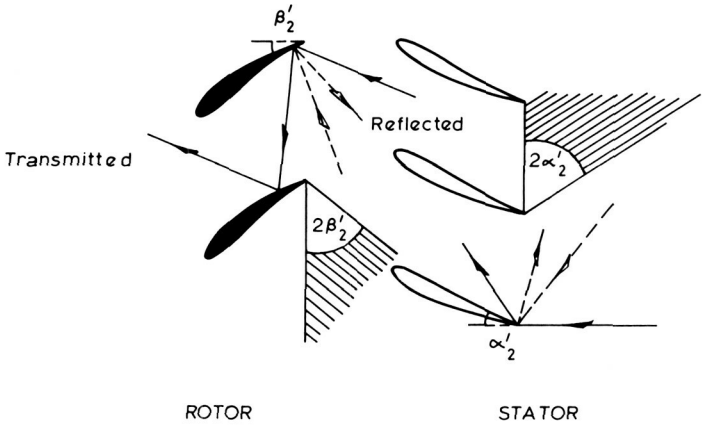

FIGURE 6.—*High-frequency sound transmission through blade rows.*

EFFECTS OF SOURCE MOTION AND MEAN FLOW

The relative amounts of broadband sound power escaping from the exhaust and inlet of a single-stage fan have been studied by Smith and House (ref. 3); they show an empirical correlation with the relative Mach number through the rotor. The same measurements have been reanalyzed for this study to give the downstream/upstream power ratio in narrow frequency bands. The tendency reported in reference 3 for more sound power to travel downstream is verified, but it appears to be restricted to

high frequencies (above 2 kHz). The high-frequency data are compared below with the predictions of a theoretical model that accounts for source motion and mean flow.

Theoretical Prediction of Downstream/Upstream Energy Split

The single blade-row model of Appendix III gives an estimate of the sound-power spectrum radiated downstream and upstream due to broadband blade forces. Provided the blades are not highly staggered (mean relative flow angle less than 30°), the downstream/upstream power ratio can be approximated to first order in Mach number by

$$\frac{1+\frac{3}{4}M_x}{1-\frac{3}{4}M_x} \tag{6}$$

The total sound-power spectrum (inlet+exhaust) is unaffected by flow to this approximation.

The energy split predicted by Appendix III actually depends on the shape of the radiated power spectrum, and equation (6) is strictly valid only for a flat spectrum of sound power in constant-percentage bands. Furthermore, the analysis is based on the assumption that many modes contribute to the sound-power spectrum at the frequency concerned. These considerations limit the application of equation (6) to frequencies around the peak of the constant-percentage-bandwidth spectrum.

Comparison of Theory with Experimental Data

Figure 7 shows the downstream/upstream power ratio for engine E, measured at three different frequencies (3.8, 7, and 11.5 kHz) over a range of axial Mach numbers. The constant-percentage broadband spectrum peaks at around 4 to 7 kHz at all speeds.

Although the data are scattered, there is a definite trend toward increasing power ratios with increasing axial Mach number, a finding which agrees fairly well with equation (6) (shown on fig. 7 as a solid line).

CONCLUSIONS

(1) Measurements of inlet-radiated broadband power spectra from a range of fans and compressors show a collapse of spectrum shape based on the estimated first-rotor wake-momentum thickness (figs. 1 and 2).

(2) A simplified model of broadband sound-power generation has been used to establish the main factors determining the radiated power, leading to the definition of a nondimensional sound-power parameter in which these factors are normalized out.

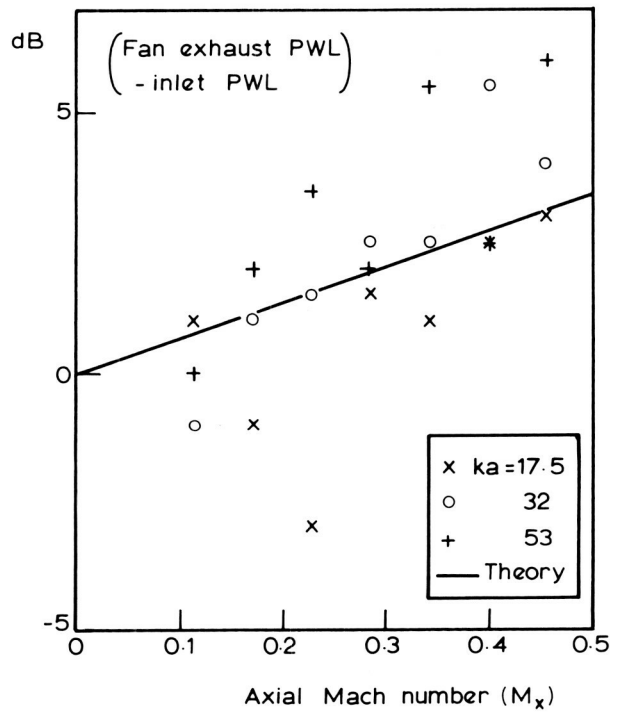

FIGURE 7.—*Ratio of exhaust to inlet sound power in narrow frequency bands—single-stage fan.*

(3) Plotting the peak (constant-percentage) power spectrum levels in normalized form collapses the data within 5 dB (fig. 3). Below a rotor relative Mach number of 0.6, the nondimensional power parameter is approximately independent of Mach number; above 0.6 there is a noticeable falloff, similar to the flow effect found by Smith and House (ref. 3).

(4) The single-stage fan levels tend to fall at the bottom of the scatter band; i.e., about 5 dB below most of the multistage points. This may well be a stage-number effect; figure 14 of reference 3 predicts differences of this order between single- and multi-stage machines over the relative Mach number range concerned (0.2 to 0.6). The difference largely disappears if the exhaust-radiated power is included in the single-stage data.

(5) Inlet directivity measurements in narrow frequency bands show a consistent trend toward more directional radiation at higher frequencies (fig. 4), which becomes more marked the larger the number of fan or compressor stages. The high-frequency beaming along the axis is, if anything, more pronounced at low engine speeds (jet noise obscures the pattern at the highest speeds) and thus cannot be explained in terms of refraction. Transmission through upstream blade rows provides a qualitative explanation.

(6) For a single-stage fan, the ratio of exhaust to inlet sound power has been measured in narrow frequency bands. Around the peak of the constant-percentage broadband power spectrum, the trend of the measurements agrees with the ratio $[1+(\frac{3}{4}M_x)]/[1-(\frac{3}{4}M_x)]$ theoretically predicted for low-stagger blade rows (fig. 7).

LIST OF SYMBOLS

a, a_0	rms radius, outer radius of annulus
b	blade chord
C_D, C_L	blade drag, lift coefficients
d	tangential spacing of blades
F	frequency parameter (L/λ)
f	frequency
$f(\beta_2,\alpha_1)$	defined in equation (9)
G	sound-power parameter, equation (5)
g	frequency exponent, equation (23)
I	acoustic intensity
k	acoustic wavenumber (ω/c)
k_y, k_z	turbulence wavenumber components (tangential, spanwise)
L	length scale, equation (3)
L_x	axial blade force per unit span
l_c	spanwise correlation length of turbulence, equation (11)
M_R, M_t	rotor Mach numbers (relative, tangential)
M_x, M_θ	flow Mach numbers (axial, peripheral)
(m,n)	annulus mode numbers (circumferential, radial)
n	number of stages in machine
S	area of duct cross section
S_R, S_R'	rotor disk area, blade area
T, T_0	absolute temperature, stagnation value
$(\Delta T_0)_n$	overall stagnation temperature rise
W, dW/df	sound power, spectral density
w	defined in equation (19)
α	turbulence intensity parameter, equation (13); axial wavenumber parameter, Appendix III
α, α'	stator flow angle, blade angle
β, β'	rotor relative flow angle, blade angle
γ	specific-heat ratio
ϵ	ratio of tangential to axial force at outer wall of duct
η_n	overall isentropic efficiency
λ	sound wavelength
ρ	fluid density
σ	blade-row solidity

ψ	angle from duct axis
ω	radian frequency (relative to swirl in Appendix IV)
ω_0, ω'	radian frequency in fixed, rotor reference frames

Subscripts

R, S	rotor, stator
1, 2	inlet, exit values for blade row
$\langle\ \rangle$	denotes time average

APPENDIX I

Generation of Broadband Acoustic Energy

Broadband noise generation is here attributed to the interaction between flow turbulence and the fan or compressor blades. More specifically, the process of sound generation at subsonic speeds is viewed in two stages: Turbulent flow produces lift fluctuations on a row of blades, and the lift fluctuations give rise to sound radiation. We shall consider the particular case where the turbulence is produced by the row of blades immediately upstream, although this is not the only possibility. The following analysis is designed to give guidelines for data correlation and is by no means a complete description of the complex processes involved.

Periodic Interaction Theory

A relatively simple case of rotor-stator interaction is that associated with the mean rotor-wake profile. Reference 1 gives the sound intensity, at any multiple of blade-passing frequency, due to a uniform axial force L_x per unit span on each stator blade at that frequency:

$$I \doteq \frac{\langle L_x^2 \rangle}{4\rho c\, d_S^2} \quad \text{(single mode, well above cutoff)} \tag{7}$$

Equation (7) is based on a two-dimensional model and assumes low-Mach-number flow. With the same assumptions, the mean-square harmonic force is given by an extension of the Kemp-Sears analysis (refs. 1 and 9) as

$$\langle L_x^2 \rangle \doteq \frac{\pi}{2} K_w \frac{\rho^2 c^5 b_S}{\omega} \sigma_R^2 C_D^2 M_R^5 f(\beta_2, \alpha_1) \tag{8}$$

where K_w is a factor allowing for the downstream decay of the rotor wakes and

$$f(\beta_2,\alpha_1) = \tan^2 \alpha_1 \frac{\cos \beta_2}{\cos \alpha_1} \cdot \sin^2 (\beta_2+\alpha_1) \cdot \left[1-\frac{C_L}{\pi} \cot (\beta_2+\alpha_1)\right]^2 \tag{9}$$

Note that the drag coefficient C_D refers to the rotor blades, and the lift coefficient C_L to the downstream stator blades. The blade-row geometry is shown in figure 8.

Application to Broadband Turbulence

The single-mode, single-frequency results given above correspond to a rotor-wake pattern that is sinusoidal in the tangential direction (i.e., single k_y wave number), uniform in the spanwise direction ($k_z=0$), and carried round with the rotor. To deal with incident turbulence that has a continuous range of wave numbers and frequencies, we use the wave-number-frequency spectrum $E(k_y, k_z, \omega)$ of the fluctuating velocity entering the stator. Only velocity components parallel to the rotor wakes (i.e., streamwise relative to the rotor) are considered here.

Figure 9 shows which regions of the turbulence spectrum give rise to propagating acoustic modes. The criterion for propagation is that for a given radian frequency ω the interaction wave number—whose components are $(k_y+2\pi s/d_S, k_z)$, where $s=\pm1, \pm2$, etc.—should be less than the acoustic wave number $k=\omega/c$. The contributing regions in the (k_y, k_z)

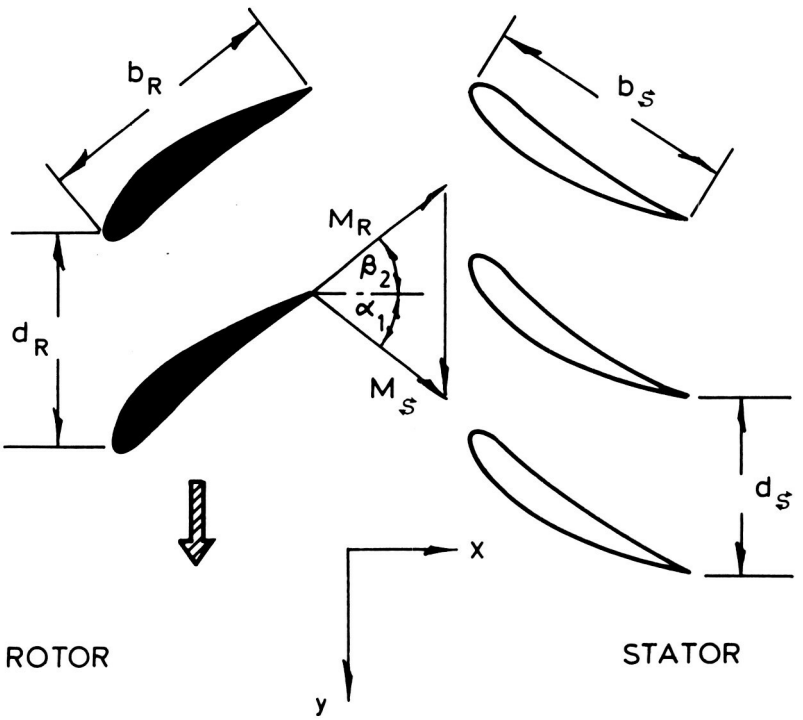

FIGURE 8.—*Geometry of rotor-stator stage.*

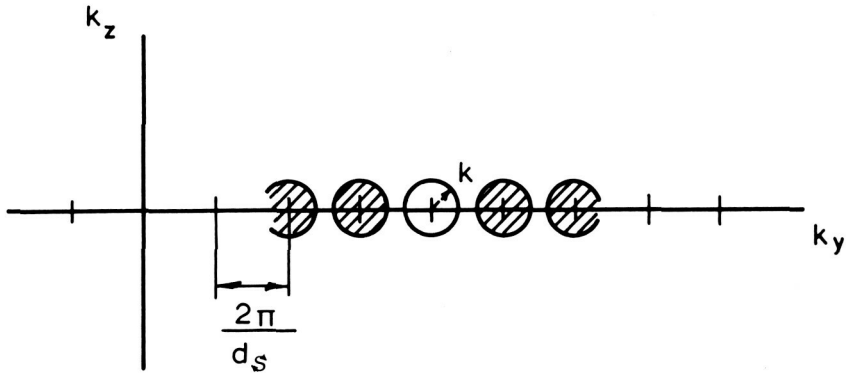

FIGURE 9.—*Regions of* (k_y,k_z) *wave-number spectrum of turbulence which contribute to sound radiation at frequency* ω.

plane are therefore circles of radius k; these overlap if the stator blades are spaced further apart than the acoustic wavelength, and are distinct regions if $d_S < \lambda/2$.

In either case, the equivalent of the mean-square harmonic wake velocity in the previous section is an integral of the wave-number spectrum over all the contributing regions. However, exact correspondence occurs only in the center of each circle; departure from two-dimensionality and proximity to cutoff introduce a weighting factor for points away from the center proportional to the axial wave number of the radiated sound[9] and, hence, proportional to the height of the hemisphere with the circle as base.

We make the following assumptions in order to estimate the wave-number integral: (1) The variation of $E(k_y,k_z,\omega)$ is small over an interval $2\pi/d_S$ in k_y; (2) the variation with k_z is small over the contributing region ($|k_z| < k$). Thus

$$E(k_y,k_z,\omega) \doteq E(k_y,0,\omega)$$

This implies that the integral length scale l_c (see below) is small compared with λ.

With these approximations, and taking account of the weighting factor mentioned above, the contributing region of the (k_y,k_z) turbulence spectrum is estimated as

$$\frac{2}{3}\pi k^2 \cdot \frac{d_S}{2\pi} \cdot 2 \int_{-\infty}^{\infty} E(k_y,0,\omega)\, dk_y \qquad (10)$$

(Note factor 2 for + and − frequencies.)

---

[9] This is an acoustic coupling factor for axial forces (see ref. 10, sec. 6.4). The aerodynamic effect of finite k_z on the fluctuating lift is shown in Appendix II to be unimportant.

If the integral length scale l_c in the spanwise direction is defined by

$$l_c = 2\pi E(k_y,0,\omega) \Big/ \int_{-\infty}^{\infty} E(k_y,k_z,\omega)\, dk_z \tag{11}$$

and the dependence of l_c on k_y is neglected, expression (10) may be written as

$$\frac{1}{6\pi} k^2 d_S l_c G(\omega) \tag{12}$$

In the above expression

$$G(\omega) = 2 \int_{-\infty}^{\infty} dk_y \int_{-\infty}^{\infty} dk_z E(k_y,k_z,\omega)$$

is the single-sided ω-spectral density of the velocity fluctuations entering the stator. A nondimensional measure of $G(\omega)$ is provided by the ratio α of $\omega G(\omega)$ to the mean-square fundamental[10] component of the rotor-wake velocity defect:

$$\alpha(\omega) = \omega G(\omega) \cdot \frac{2}{c^2 \sigma_R^2 C_D^2 M_x^2} \tag{13}$$

It follows from equations (12) and (13) that, in order to apply the periodic-wake analysis to the present problem, it is simply necessary to replace K_w in equation (8) by

$$\frac{1}{6\pi} k^2 d_S l_c \cdot \frac{\alpha}{\omega} \tag{14}$$

This, with equation (7), gives the acoustic intensity per unit bandwidth due to axial lift forces on the stator blades as

$$\frac{dI}{d\omega} = \frac{1}{48} \alpha \rho c^2 l_c \sigma_S \sigma_R^2 C_D^2 M_R^5 f(\beta_2,\alpha_1) \tag{15}$$

with $l_c \ll \lambda$.

The opposite extreme to equation (15) is obtained when the spanwise integral length scale is greater than λ; a similar analysis then gives

$$\frac{dI}{d\omega} = \frac{\pi}{32} \alpha \rho c^3 \cdot \frac{1}{\omega} \sigma_S \sigma_R^2 C_D^2 M_R^5 f(\beta_2,\alpha_1) \tag{16}$$

with $l_c > \lambda$.

---

[10] i.e., with period equal to the rotor blade space.

Radiation from Turbulent Boundary-Layer Pressure Fluctuations

In the preceding analysis, blade lift fluctuations are attributed to incident turbulence. An alternative cause of lift fluctuations is the unsteady pressure field set up by the blade's own turbulent boundary layer and wake. This mechanism was recognized by Kramer (ref. 11), and a quantitative estimate of the sound radiation was made by Sharland (ref. 12) using theoretical ideas put forward by Lilley (ref. 13). In fact the simplified sound power parameter, equation (5), used to correlate the data does not distinguish between the two mechanisms. The question, whether the rotor-generated turbulence radiates by interaction with the rotor or the downstream stator, is therefore left open.

APPENDIX II

Three-Dimensional Effects on Fluctuating Lift

Mugridge (ref. 6) has estimated the fluctuating lift per unit span on a two-dimensional airfoil in a three-dimensional convected gust pattern by considering a single radian frequency ω and spanwise wavenumber k_z. The case $k_z=0$ corresponds to Sears' two-dimensional analysis (ref. 9).

The mean-square fluctuating lift is approximately equal to the two-dimensional mean-square lift multiplied by a correction factor

$$\left(1+\frac{p^2}{n^2+2/\pi^2}\right)^{-1}$$

with $p^2+n^2<4$, where $n=\omega b/2U$ (i.e., the reduced frequency) and $p=\frac{1}{2}k_z b$.

Since $p/n=k_z U/\omega$, and we are interested only in values of k_z less than k for sound radiation, it follows that over this range $p<Mn$ with $M=U/c$. This limits the correction factor above to between $\frac{1}{2}$ and 1 for subsonic flow.

For high gust wavenumbers, a more accurate value of the correction factor is available from an independent analysis by Filotas (ref. 14); it is

$$\frac{2}{\pi p}\,(1+p^2/n^2)^{-1/2}$$

with $p^2>4$, $n>1$.

Large values of p will be associated in the present problem with acoustic wavelengths that are small compared with the blade chord (i.e., high frequencies). However, the acoustic representation of the blade as a line force breaks down in this region.

APPENDIX III

Downstream/Upstream Energy Split from an Isolated Blade Row

Apart from any reflecting surfaces upstream or downstream, a rotating blade row is expected to radiate different amounts of sound power in the upstream and downstream directions. Both the source motion and mean flow contribute to this effect, which applies both to discrete-frequency[11] and broadband radiation. The following analysis deals with the broadband case.

For this purpose the blade row is modeled by a force distribution at one cross section of a uniform axisymmetric duct. The local force per unit area has components (f_x, f_θ, f_r) in the axial, tangential, and radial directions, and we assume for simplicity that

$$f_\theta = \epsilon \left(\frac{r}{a_0}\right) f_x \tag{17}$$

with $f_r = 0$. (a_0 is the outer radius of the annular cross section.) A swirling mean flow in the duct is modeled by a uniform axial Mach number M_x together with a solid-body rotation.

The analysis starts from the result derived in reference 16, section 4, for single-frequency excitation in a single (m,n) duct mode. This gives the downstream (W_+) and upstream (W_-) sound power in terms of the axial-force modal amplitude $\bar{F}_x$, as

$$W_\pm(m,n) = \frac{1}{8}\frac{\omega_0}{\omega}\frac{|\bar{F}_x|^2 S}{\alpha\rho c} A_\pm$$

and

$$A_\pm = \left[\frac{\pm\alpha - M_x + (\omega_0/\omega)(m\epsilon/w)(1-M_x^2)}{1 \mp \alpha M_x}\right]^2 \tag{18}$$

Here α is the axial wavenumber parameter, defined in equation (24) below; $\omega_0 = wc/a_0$ is the fixed-frame radian frequency, and ω is the corresponding frequency relative to the swirl. Equation (18) is valid over the whole frequency range above mode cutoff.

Frequency Relationships

If the swirl angular velocity is Ω in the θ direction, ω is related to ω_0 by

$$\omega = \omega_0 - m\Omega \qquad (m = \text{circumferential mode number})$$

---

[11] The discrete-frequency case has been studied theoretically and checked against experimental data by Mani (ref. 15).

Thus

$$\frac{\omega}{\omega_0} = 1 - \frac{m}{w} M_\theta \tag{19}$$

where

$$w = \frac{\omega_0 a_0}{c} \qquad \text{(based on fixed-frame frequency)}$$

and

$$M_\theta = \frac{\Omega a_0}{c}$$

is the peripheral swirl Mach number.

Similarly the radian frequency ω' in the rotor frame of reference is related to ω_0 by

$$\frac{\omega'}{\omega_0} = 1 - \frac{m}{w} M_t \tag{20}$$

where M_t is the rotor tip Mach number.

Broadband Excitation

Since ω_0 and ω' are related by a constant factor for a given m value, the single-frequency sound-power result (eq. (18)) can be generalized to broadband excitation by the substitutions

$$\left.\begin{aligned} \tfrac{1}{2} \mid \bar{F}_x \mid^2 &\rightarrow \omega' G_x(\omega') \\ W_\pm(m,n) &\rightarrow \omega_0 \frac{dW_\pm(m,n)}{d\omega_0} \end{aligned}\right\} \tag{21}$$

Thus

$$\frac{dW_\pm(m,n)}{d\omega_0} = \frac{1}{4} \frac{S}{\alpha \rho c} \frac{\omega'}{\omega} G_x(\omega') \cdot A_\pm \tag{22}$$

If the force spectral density $G_x(\omega')$ varies as $(\omega')^g$, equation (22) can be written as

$$\frac{dW_\pm(m,n)}{d\omega_0} = \frac{1}{4} \frac{S}{\alpha \rho c} \left(\frac{\omega}{\omega_0}\right)^{-1} \left(\frac{\omega'}{\omega_0}\right)^{g+1} G_x(\omega_0) \cdot A_\pm \tag{23}$$

Cutoff Condition

We consider only $(m,0)$ modes, for which

$$\alpha \doteq \left[1-(1-M_x^2)\left(\frac{mc}{a_0\omega}\right)^2\right]^{1/2} \tag{24}$$

Cutoff occurs when

$$\left(\frac{mc}{a_0\omega}\right)^2(1-M_x^2)=1$$

i.e., from equation (19),

$$\left(\frac{m}{w}\right)^2(1-M_x^2)=\left(1-\frac{m}{w}M_\theta\right)^2$$

Thus the propagation range is given by

$$\frac{-M_\theta-(1-M_x^2)^{1/2}}{1-M^2}\leq\frac{m}{w}\leq\frac{-M_\theta+(1-M_x^2)^{1/2}}{1-M^2} \tag{25}$$

with $M^2=M_x^2+M_\theta^2$. Modes within this range will propagate along the duct; modes outside the range make no contribution to the sound power in the present model.

The substitution

$$\frac{m}{w}=\frac{-M_\theta}{1-M^2}+\frac{(1-M_x^2)^{1/2}}{1-M^2}\sin\phi \tag{26}$$

gives the propagation range in terms of ϕ as $-\frac{1}{2}\pi\leq\phi\leq\frac{1}{2}\pi$. Also, α is given by

$$\alpha=\frac{\omega_0}{\omega}(1-M^2)^{1/2}(1-M_x^2)^{1/2}\cos\phi \tag{27}$$

Summation over Propagating Modes

The total sound power per unit bandwidth $dW_\pm/d\omega_0$, radiated in either direction, is found by summing the contributions given by equation (22) for all propagating modes. Two simplifying assumptions are introduced at this point.

(1) The excitation spectral density G_x is taken as the same for all $(m,0)$ modes and as zero for all higher order radial modes. Although it would probably be more realistic to assign equal excitation to all modes regardless of radial order, the exclusion of higher order modes is not expected to alter the downstream/upstream energy split significantly.

(2) The propagation range is assumed to contain a large enough number of $(m,0)$ modes that the discrete summation over integer m values can be replaced by integration over a continuous range. The multimode sound power in either direction is then

$$\left.\begin{aligned}\frac{dW_{\pm}}{d\omega_0} &\doteq \int_{m_1}^{m_2} \frac{dW_{\pm}(m,0)}{d\omega_0}\, dm \\ &= \frac{w(1-M_x^2)^{1/2}}{1-M^2} \int_{-\pi/2}^{\pi/2} \frac{dW_{\pm}(m,0)}{d\omega_0} \cos\phi \cdot d\phi\end{aligned}\right\} \tag{28}$$

The integral over ϕ in equation (28) is a function of ϵ, M_x, M_θ, and M_t; it can be evaluated using equations (18), (23), (26), and (27). A particularly simple result, valid for low Mach numbers, is obtained by neglecting squares and higher powers of the various Mach numbers; to this accuracy,

$$\frac{dW_{\pm}}{d\omega_0} \doteq \frac{1}{4}\frac{S}{\rho c} w\, G_x(\omega_0) \cdot \left\{\tfrac{1}{2}\pi\,(1+\epsilon^2) \mp \frac{4}{3}\left[(1-\epsilon^2)\,M_x + \epsilon\, M_\theta + (g+1)\,\epsilon M_t\right]\right\} \tag{29}$$

Special Case: Force Perpendicular to Relative Mean Flow

If the fluctuating blade forces act in the lift direction (i.e., perpendicular to the relative flow), then

$$\epsilon = \cot\beta_m = \frac{M_x}{M_t - M_\theta} \tag{30}$$

where β_m is the mean relative flow angle referred to the axis. Combining this relation with equation (29), and taking the exponent g as -2, gives

$$\frac{dW_+/d\omega_0}{dW_-/d\omega_0} \doteq \frac{1+(8/3\pi)M_x\cos^2\beta_m}{1-(8/3\pi)M_x\cos^2\beta_m} \tag{31}$$

The assumption $g=-2$ corresponds, according to equation (29), to a flat spectrum of sound power in constant-percentage bands.

A noteworthy feature of equation (31) is that, provided β_m is not more than 30°, the downstream/upstream sound power ratio is almost independent of β_m and can be approximated by

$$\frac{1+\frac{3}{4}M_x}{1-\frac{3}{4}M_x} \tag{32}$$

In other words, the energy split is determined solely by the axial Mach number and is the same for both rotating and stationary blades, provided the relative flow angles are not too large.

REFERENCES

1. Morfey, C. L., *Sound Generation in Subsonic Turbomachinery.* ASME Paper 69–WA/FE–4, 1969. (See *Trans. ASME, J. Basic Eng.*, Vol. 92D, 1970, p. 450.)
2. Lighthill, M. J., On Sound Generated Aerodynamically: I. General Theory. *Proc. Roy. Soc. (London)*, Series A, Vol. 211, 1952, p. 564.
3. Smith, M. J. T., and M. E. House, Internally Generated Noise From Gas Turbine Engines: Measurement and Prediction. *Trans. ASME, J. Eng. for Power*, Vol. 89A, 1967, p. 177.
4. Morfey, C. L., and H. Dawson, *Axial Compressor Noise: Some Results From Aero-Engine Research.* Bristol-Siddeley Engines Ltd., TRH 107, 1966.
5. Snow, R., M.S. thesis, Inst. Sound and Vib. Res., Southampton U., 1970.
6. Mugridge, B. D., Ph.D. dissertation, Southampton U., 1970. (See *J. Sound Vib.*, Vol. 18, 1971, p. 475.)
7. Lieblein, S., and W. H. Roudebush, *Theoretical Loss Relations for Low-Speed Two-Dimensional-Cascade Flow.* NACA Technical Note 3662, 1956.
8. Morfey, C. L., A Review of the Sound-Generating Mechanisms in Aircraft-Engine Fans and Compressors. *Proc. UTIAS/AFOSR Symposium on Aerodynamic Noise*, H. S. Ribner, ed., Toronto U. Press, 1969, p. 299.
9. Kemp, N. H., On the Lift and Circulation of Airfoils in Some Unsteady-Flow Problems. *J. Aero. Sci.*, Vol. 19, 1952, p. 713.
10. Morfey, C. L., Rotating Pressure Patterns in Ducts: Their Generation and Transmission. *J. Sound Vib.*, Vol. 1, 1964, p. 60.
11. Kramer, M., The Aerodynamic Profile as Acoustic Noise Generator. *J. Aero. Sci.*, Vol. 20, 1953, p. 280.
12. Sharland, I. J., Sources of Noise in Axial Flow Fans. *J. Sound Vib.*, Vol. 1, 1964, p. 302.
13. Lilley, G. M., *On the Vortex Noise From Airscrews, Fans and Compressors.* Rolls Royce Ltd., Noise Panel Report, 1961.
14. Filotas, L. T., Response of an Infinite Wing to an Oblique Sinusoidal Gust. *Basic Aerodynamic Noise Research*, I. R. Schwartz, ed., NASA SP–207, 1969.
15. Mani, R., Discrete Frequency Noise Generation From an Axial Flow Fan Blade Row. *Trans. ASME, J. Basic Eng.*, Vol. 92D, 1970, p. 37.
16. Morfey, C. L., Ph.D. dissertation, Southampton U., 1970. (see *J. Sound Vib.*, Vol. 14, 1971, p. 37.)

DISCUSSION

M. V. LOWSON (Loughborough University, England): This interesting paper by Dr. Morfey raises a number of points which deserve further discussion. It is assumed in the paper that shed turbulence is the principal source of broadband noise radiation. While this is certainly an important contributor, other sources can also give rise to broadband noise. The turbulence in the inlet boundary layer of a jet engine is probably much larger, in both scale and level, than that of the standard equilibrium boundary layer, and also interacts with the highest speed part of the rotor near the tip. Indeed the tip itself can be regarded as running in a stalled condition, and the direct self-induced radiation at the tip could well be large. Definitive measurements of inlet turbulence levels and spectra are badly needed to illuminate this problem.

The empirical correlation on momentum thickness demonstrated by Morfey offers some evidence in favor of the dominance of shed turbulence effects, but it should be pointed out that, because all engines are designed to similar rules, empirical parameters tend to move together. Thus there is some danger in inferring source mechanisms from the success of empirical collapses.

The measured high-frequency beaming of the broadband noise is an interesting effect, particularly since it is more pronounced than predicted by the theory. A possible reason for this is that the theoretical estimates ascribe too high a level to the higher order circumferential and radial modes. The actual source strength must fall off smoothly toward the tip and this would cause a lower level of the higher order radial modes than the rectangular distribution assumed. Since it is these higher order modes which cause the radiation normal to the axis, a somewhat lower level of sideline radiation than that of the present theory can be anticipated.

As a final point, I wonder if Dr. Morfey would care to indicate his present thoughts on the likely relative significance of the dipole and quadrupole source mechanisms for broadband noise radiation.

M. E. HOUSE (Southampton University): Dr. Morfey is well recognized for his theoretical contribution to the problems of turbomachinery noise, and indeed his paper presented at the 1969 Winter Annual Meeting of ASME held at Los Angeles, California (ref. 1), contains a very full

treatment of subsonic rotor-stator interaction noise in terms of steady-state parameters. I must confess, however, to being a little disappointed that that paper offered no experimental verification.

His present paper extends the concepts to the case of random or broadband sound, and here I am pleased to note that experimental data are included.

I have little or no comment to make on the derivations in the paper or the appendixes since they follow logically from the basis and assumptions stated by Dr. Morfey. My main concern lies within these assumptions.

First, I would like to comment on sound-power normalization. As for discrete tones, there are numerous mechanisms which one can postulate as giving rise to random noise from compressors. While I, myself, and others, have pointed to the likely dominances of one or another mechanism for a particular class of machine operating in particular circumstances, it is unlikely that this will hold universally. Rather there will be transition regimes in which a given mechanism gives way to a stronger one. Evidence of this is well known in the case of transonic compressor discrete tone noise when conditions are reached where rotor-associated force fields may propagate and dominate the conventional rotor-stator interaction tones. Dr. Morfey has elected to inspect the broadband noise from a wide range of compressors (table I of his paper) in terms of frequency scaling using a length scale associated with the rotor blade momentum thickness. The sound-power level normalizing technique he uses is also heavily dependent upon the mechanism of lift fluctuations over blade surfaces caused by turbulence wakes from upstream rows.

While this approach might be realistic for multistage compressors (say three stages and above), work done over the last 2 to 3 years at Rolls-Royce (ref. D–1) indicates that for subsonic single-stage fans, at least, other mechanisms can and do strongly influence the radiated sound characteristics. These include blade interactions with the turbulence structure of the intake flow. I would not, therefore, expect Dr. Morfey's normalizing functions to cope with both multi- and single-stage machines, and perhaps this is another reason for the tendency of the engine E data to fall at the lower scatter band.

Another subject I wish to discuss is frequency resolution of data. The data in figure 2 of reference 5 used by Morfey were frequency-analyzed using 100-Hz Spectral Dynamics equipment with approximately 2-second averaging (from the 15 ips recorded data on a 30-in. tape loop).

It is interesting to inspect such data with even greater resolution and averaging. An example is the Rolls-Royce Conway compressor noise for a well-subsonic operating condition, as shown in figure D–1, where 20-Hz Spectral Dynamics equipment was used with 7-second averaging. Besides the "sum-and-difference" tones of the type noted by Crigler, et al. (ref. D–2), the signal clearly contains a large range of tones at compressor

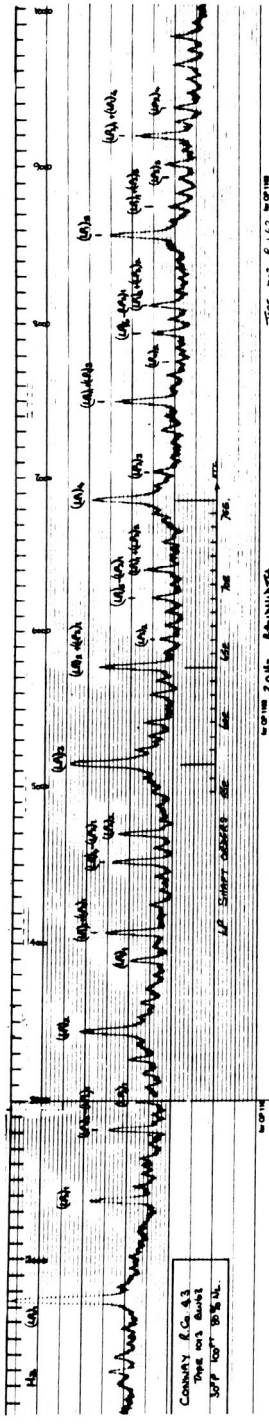

FIGURE D–1.—*20-Hz constant bandwidth spectrum of typical subsonic multistage compressor forward arc noise.*

shaft orders. Most of these protrude less than 5 dB and hence would appear much as the data of Snow (ref. 5) when resolved to only 100 Hz.

The data for engines—A, B, C, and D being of 5-percent bandwidth—would also fail to resolve adequately the compressor shaft order signals.

Although I do not agree that the sound-power level data collapse obtained by Morfey is a significant improvement on past attempts, his correlation does, however, seem reasonable. Nevertheless I feel that in view of my comments above this can only be fortuitous. The directivity data collapse, is, however, surprisingly good and I wonder whether Dr. Morfey would agree that this could be due to a much closer association with discrete tone characteristics than he had assumed.

Finally, I would like to comment on Dr. Morfey's optical model for high-frequency directivity. A marked difference noted in directivity between the single-stage data and the remaining engines is interesting. Dr. Morfey has developed a simple optical model to explain this, but I wonder if he has attempted to use the approaches of Kaji and Mani (refs. 15, D–3). The neglect of flow-associated effects on the propagation of sound through blade rows seems unwarranted and I feel that one needs an integral approach to the problems of Dr. Morfey's sections entitled "Optical Model for High-Frequency Directivity" and "Effects of Source Motion and Mean Flow." I also feel that the effect of blade spanwise twist cannot be ignored since conditions may not be such as to prevent transmission over the entire compressor annulus.

R. MANI (University of Massachusetts): The paper is an elegant contribution to the broadband noise problem in turbomachines. It should prove particularly useful as a guide to experimental work. In contrast to earlier works on the subject, while the author uses similarity arguments as the need arises, there is a welcome emphasis on use of first principles in computing the sound power, directivity, energy split, etc. The following are some more specific comments:

(1) In the theoretical development the effect of longitudinal (chordwise) velocity fluctuation is included resulting in a C_L term in $f(\beta_2, \alpha_1)$. In computing the sound-power parameter G, the C_L term was dropped. Now in the Smith-House paper, the authors explain the higher normalized sound power at part speed as due to the cascade operating at lower incidence angle and hence in regimes of higher lift-curve slope. The Smith and House argument is based on quasi-steady, real fluid effects and I wonder if the retention of the C_L term in $f(\beta_2, \alpha_1)$ does not provide a more natural explanation, based on unsteady airfoil theory, of the trends observed by Smith and House.

(2) With regard to the optical model for transmission through blade rows, the mechanism by which a blade row produces reflected and transmitted waves is different from the one suggested by figure 6. The blade

row behaves like a pair of line diffraction gratings coupled by parallel-plate waveguides. The reflected and transmitted waves have orientations given by the Tyler-Sofrin formula that the tangential wave number k_y of these waves differs from that of the incident wave by an integer multiple of $(2\pi/d)$, being the tangential spacing of the blade row. Thus blade rows of completely different stagger angles but of the same tangential spacing would give the same orientations of reflected and transmitted waves. Actually, at high frequencies the effects are more complex than at low frequencies since several higher order transmitted and reflected waves are produced. Based on some calculations that I have done on this problem, I did conclude that the author's surmise, to wit that the acoustic energy transmission coefficients are low in the incidence regions shown shaded in figure 6, is probably correct. I believe, however, that the mechanism involved here is that the degradation of acoustic energy to wake kinetic energy (always present in such a problem when moving medium effects are involved) is high in these incidence regimes at high frequencies.

(3) To students of the theoretical aspects of the subject, attention is specially directed to the appendixes, where considerations involved in the transition from the discrete-frequency to the continuous-spectrum case are comprehensively dealt with.

(4) I agree with the author's approach of gradually building the refinements into the analysis. Examples are extension of the Kemp-Sears work to include chordwise velocity fluctuations and the effect of the cutoff weighting factor on the acoustic efficiency of axial fluctuating forces, etc. Perhaps the author will agree that there are further refinements not mentioned here which could be significant. Two examples with regard to sound-power estimation are that tangential fluctuating forces would make a contribution near cutoff and, secondly, work on estimation of unsteady blade forces suggests that Kemp-Sears type estimates are rather inadequate near cutoff.

MORFEY (author): The discussers raise a number of interesting points and I am grateful for their comments. Since the questions mainly fall in the three categories used by Mr. House, I have grouped my replies under these headings.

I will first address the subject of sound-power normalization. The fact that the single-stage fan (E) falls on the lower edge of the scatter band (fig. 3) might well be accounted for by a difference in source mechanisms, as Mr. House suggests. Figure 2 shows that, compared with the multistage machines, the mean spectrum shape for engine E is deficient at high frequencies.

Dr. Mani's point about the C_L effect in $f(\beta_2,\alpha_1)$ deserves further study. Retention of the C_L term would raise the normalized level of engine E at maximum speed by around 5 dB. Because this machine is a single-stage

fan, however, the correction may not be much different over the whole speed range. Probably a more important reason for the failure to follow a V^6 speed variation (as noted in ref. 3) is the breakdown of Strouhal number scaling in the frequency spectrum.

Dr. Lowson's final question is also relevant to the normalization procedure. A comparison of the dipole and quadrupole mechanisms—with a number of simplifying assumptions—has been made for the related problem of an isolated rotor in nonuniform flow (see Paper D3, Loughborough Symposium on Aerodynamic Noise, September 1970). If one adopts the Kemp-Sears method (ref. 9) of calculating the unsteady blade forces, the comparison shows that dipole noise is likely to predominate unless the rotor pressure ratio exceeds 1.1. However, this conclusion may have to be modified as theory and experiment yield more data on the interaction of blade rows with turbulent flow.[12]

The second subject I will reply to is frequency resolution of the data. This is a key question which has not been satisfactorily resolved in published data, and the danger of even 100-Hz bandwidth analysis is well illustrated by the Conway spectrum. In fact the engine E data used in the paper were analyzed initially at 20 Hz, and no shaft order tones were detectable at this bandwidth. Nevertheless, the possibility remains that the spectra consist of overlapping peaks centered at multiples of shaft rotation frequency. These peaks would arise, of course, from irregularities in blade geometry or spacing round the rotor disk.

Mr. House suggests that such "semiordered" noise would show a better directivity collapse than true broadband noise; but the evidence from tone radiation patterns (ref. 8) indicates that the more ordered the source the less correlation there is between engines.

Finally, I wish to reply to comments made concerning the optical model for high-frequency directivity. It would be interesting to take Dr. Mani's theory on sound transmission through blade rows and apply it at very high frequencies. I would expect, as he suggests, that the wave theory would support the trend predicted by the optical model. If this is the case, it might be worth extending the optical model to include the effects of flow and blade twist, as indicated by Mr. House.

---

[12] (Note added in proof) Substantial advances have been made, since this paper was presented, in understanding the radiation of sound from blades in turbulent flow. Reference D-4 gives an updated review of the situation; it is arguable that the spectrum collapse on L/λ should be replaced by a collapse on rotor chord/wavelength.

REFERENCES

D–1. Barry, B., and C. J. Moore, *Subsonic Fan Noise.* Paper to be presented at Symposium on Aerodynamic Noise, Loughborough U., England, September 14–17, 1970. (See *J. Sound Vib.*, Vol. 17, 1971, p. 207)

D–2. Crigler, J. L., W. L. Copeland, and G. J. Morris, *Noise Studies to Evaluate Effects of IGV-Rotor Spacing.* NASA TN D-4690, 1968.

D–3. Kaji, S., *Axial-Flow Compressor Noise.* Ph.D. dissertation, Tokyo U., 1969. (See *J. Sound Vib.*, Vol. 11, 1970, p. 355)

D–4. Morfey, C. L., Rotating Blades and Aerodynamic Sound. *J. Sound Vib.*, Vol. 28, 1973, p. 587.